incubated at 22°C for 20 min before it was viewed by fluorescence microscopy.
16. T. Kouyama and K. Mihashi, *Eur. J. Biochem.* **114**, 33 (1981); J. A. Cooper, S. B. Walker, T. D. Pollard, *J. Muscle Res. Cell Motil.* **4**, 253 (1983).
17. The pyrene-actin assay measures the weight concentration of polymer over time and is not sensitive to the distribution of filament lengths (*16*). Pyrene-actin was prepared as described in (*16*). Pyrene-labeled G-actin and unlabeled G-actin were isolated by centrifuging actin in G-buffer at 228,000*g* for 15 min to remove F-actin. For polymerization reactions, the Arp2/3 complex, ActA-His, and/or ActA-N-His were mixed and brought to 5 μl in control buffer [20 mM Mops (pH 7.0), 100 mM KCl, 2 mM $MgCl_2$, 5 mM EGTA, 1 mM EDTA, 0.2 mM ATP, 0.5 mM DTT, 10% (v/v) glycerol]. This solution was immediately mixed with 5 μl of 10× initiation buffer (20 mM $MgCl_2$, 10 mM EGTA, 5 mM ATP) and immediately added to 40 μl of G-actin solution (90% unlabeled actin and 10% pyrene-actin in G-buffer) to initiate polymerization. To monitor actin depolymerization, 7 μM pyrene G-actin was polymerized for 4 to 5 hours at 20°C by adding 10× initiation buffer (20 mM $MgCl_2$, 10 mM EGTA, 5 mM ATP). Depolymerization was initiated by diluting 2 μl of F-actin into 48 μl of G-buffer containing 1 μl of control buffer or 1 μl of 6.4 μM Arp2/3 complex in control buffer (0.27 μM actin, 0.13 μM Arp2/3). Pyrene fluorescence was monitored with a fluorometer (excitation wavelength, 365 nm; emission wavelength, 407 nm).
18. I. Lasa *et al.*, *EMBO J.* **16**, 1531 (1997).
19. To generate ActA-His, a truncated *actA* gene encoding amino acids 1 to 613 but lacking the transmembrane domain was amplified by polymerase chain reaction (PCR). Primers used were GGAAGCTTGTGGATGCTTCTGAAAGTGAC (upstream of the *actA* promoter) and GGGGATCCCGTCGTATGGTTCCCTGG (bases 1812 to 1839 of *actA*; Bam HI site is underlined). The PCR product was digested with Bam HI and Hin dIII (site upstream of promoter) and was subcloned into pAM401, yielding pDP2683. To introduce the His_6 tag, the Bam HI–Xba I fragment of pQE-60 (Qiagen) encoding amino acids GSRSHHHHHH (G, Gly; S, Ser, R, Arg; H, His) was subcloned into pDP2683 to yield pDP2717. This was transformed into *L. monocytogenes* strain DPL1545 (*6*) to yield strain DPL2723. To generate ActA-N-His, a fragment of *actA* encoding amino acids 1 to 263 was amplified by PCR. Primers used were CGGGATCCTGAAGCTTGGGAAGCAG (upstream of *actA* promoter; Bam HI site underlined) and GCTCTAGATTAGTGGTGGTGGTGGTGCGAAGCATTTACCTCTTCACT (bases 769 to 789 of *actA*; Xba I site underlined), which encodes the His_6 tag. The PCR product was digested with Bam HI and Xba I and ligated into pAM401 to yield pDP3624. This was transformed into *L. monocytogenes* strain DPL1545 to yield strain DPL3625. Secreted ActA-His and ActA-N-His were purified from culture media; 475 ml of brain heart infusion media containing chloramphenicol (10 μg/ml) (BHI cm10) was inoculated with 25-ml overnight cultures of strain DPL2723 or DPL3625 in BHI cm10 and was grown at 37°C for 6 to 8 hours. After bacteria were pelleted, protein was precipitated from the supernatant by adding ammonium sulfate to 40% (ActA-His) or 60% (ActA-N-His) saturation. Precipitated protein was resuspended in binding buffer [20 mM Mops (pH 7.0), 100 mM KCl, 20 mM imidazole (pH 7.0)] and bound to 0.5 ml of nickel nitrilotriacetic acid (Ni-NTA) agarose resin (Qiagen). The resin was washed with binding buffer and proteins were eluted with elution buffer [20 mM Mops (pH 7.0), 100 mM KCl, 250 mM imidazole (pH 7.0)]. Eluted proteins were further purified by Superose-6 (Pharmacia) gel-filtration chromatography in control buffer for the pyrene-actin experiments (*17*) and were frozen in N_2(l) and stored at −80°C.
20. C. E. Walczak, S. Verma, T. J. Mitchison, *J. Cell Biol.* **136**, 859 (1997). His-XCTK2 tail alone (20 nM) had no effect on the polymerization of 2 μM actin in the pyrene-actin assay (*17*).
21. For electron microscopy, ActA-His (70 nM) and/or Arp2/3 complex (70 nM) were mixed with 10 μl of 2× polymerization buffer [100 mM KCl, 20 mM imidazole (pH 7.0), 2 mM EGTA, 2 mM $MgCl_2$] and immediately added to 10 μl of 5 μM G-actin (in G-buffer containing 0.5 mM ATP). After polymerizing for 30 s, 2 μl of actin mix was spotted onto Formvar-coated glow-discharged grids (Pellco), washed with 1× polymerization buffer and distilled H_2O, and negatively stained with 1% uranyl acetate in 50% methanol. At higher actin concentrations or longer polymerization times, some filaments were observed in all reaction mixtures, although more filaments were consistently observed in reaction mixtures containing both the Arp2/3 complex and ActA.
22. L. G. Tilney, D. J. DeRosier, M. S. Tilney, *J. Cell Biol.* **118**, 71 (1992); L. G. Tilney, D. J. DeRosier, A. Weber, M. S. Tilney, *ibid.* p. 83.
23. J. A. Cooper, *ibid.* **105**, 1473 (1987).
24. S. Pistor, T. Chakraborty, U. Walter, J. Wehland, *Curr. Biol.* **5**, 517 (1995); I. Lasa, V. David, E. Gouin, J. B. Marchand, P. Cossart, *Mol. Microbiol.* **18**, 425 (1995).
25. G. A. Smith, J. A. Theriot, D. A. Portnoy, *J. Cell Biol.* **135**, 647 (1996).
26. T. Chakraborty *et al.*, *EMBO J.* **14**, 1314 (1995); F. B. Gertler, K. Niebuhr, M. Reinhard, J. Wehland, P. Soriano, *Cell* **87**, 227 (1996); M. Reinhard *et al.*, *EMBO J.* **14**, 1583 (1995).
27. J. A. Theriot, J. Rosenblatt, D. A. Portnoy, C. P. Goldschmidt, T. J. Mitchison, *Cell* **76**, 505 (1994); J. B. Marchand *et al.*, *J. Cell Biol.* **130**, 331 (1995).
28. P. Mourrain *et al.*, *Proc. Natl. Acad. Sci. U.S.A.* **94**, 10034 (1997).
29. We are indebted to G. Smith for help and advice on generating secreted derivatives of ActA. We thank M. Moritz and C. Walczak for comments on the manuscript. Supported by grants from the NIH to T.J.M. (GM48027) and D.A.P. (AI26919). M.D.W. is a Leukemia Society of America Special Fellow.

1 April 1998; accepted 29 May 1998

Congenital Heart Disease Caused by Mutations in the Transcription Factor *NKX2-5*

Jean-Jacques Schott,* D. Woodrow Benson,*† Craig T. Basson,‡ William Pease, G. Michael Silberbach, Jeffrey P. Moak, Barry J. Maron, Christine E. Seidman, J. G. Seidman§

Mutations in the gene encoding the homeobox transcription factor NKX2-5 were found to cause nonsyndromic, human congenital heart disease. A dominant disease locus associated with cardiac malformations and atrioventricular conduction abnormalities was mapped to chromosome 5q35, where *NKX2-5*, a *Drosophila tinman* homolog, is located. Three different *NKX2-5* mutations were identified. Two are predicted to impair binding of NKX2-5 to target DNA, resulting in haploinsufficiency, and a third potentially augments target-DNA binding. These data indicate that NKX2-5 is important for regulation of septation during cardiac morphogenesis and for maturation and maintenance of atrioventricular node function throughout life.

Cardiac development is a complex biological process requiring the integration of cell commitment, morphogenesis, and excitation-contraction coupling (*1, 2*). Several transcription factors (*3*) have been implicated in this process on the basis of their spatial and temporal patterns of expression or their phenotypic effects when they are functionally inactivated in flies or mice. Analyses of the *tinman* gene in *Drosophila melanogaster*, which encodes a homeobox transcription factor, indicate that it has an essential role for specification of heart muscle progenitors in nascent mesoderm (*4*). Targeted disruption of a murine homolog of *tinman*, *Nkx2.5*, causes early embryonic lethality (*5*), with cardiac development arrested at the linear heart tube stage, prior to looping. Cardiac expression of *Nkx2.5* continues throughout development and into adult life (*6*), but the functions regulated by its continued expression are unknown.

Identification of human mutations that cause congenital heart disease offers a complementary approach to gene ablation studies and particularly fosters definition of gene defects that perturb later stages of cardiac development. Cardiac septation is a critical morphogenetic process in which the primordial single atrium and ventricle are partitioned into four chambers. Mistakes in this process occur commonly in humans; 1 in 1500 live births have an atrial septal defect

J.-J. Schott and J. G. Seidman, Department of Genetics and Howard Hughes Medical Institute, Harvard Medical School, Boston, MA 02115, USA. D. W. Benson, C. T. Basson, C. E. Seidman, Cardiovascular Division and Howard Hughes Medical Institute, Brigham and Women's Hospital, Boston, MA 02115, USA. W. Pease, Harrisburg Hospital, Harrisburg, PA 17104, USA. G. M. Silberbach, Division of Pediatric Cardiology, Oregon Health Science University, Portland, OR 97201, USA. J. P. Moak, Division of Pediatric Cardiology, Children's National Medical Center, Washington, DC 20010, USA. B. J. Maron, Minneapolis Heart Institute Foundation, Minneapolis, MN 55407, USA.

*These authors contributed equally to this work.
†Present address: Cardiovascular Genetics, Medical University of South Carolina, Charleston, SC 29451, USA.
‡Present address: Cardiovascular Division, Cornell University Medical College, New York, NY 10021, USA.
§To whom correspondence should be addressed. E-mail: seidman@rascal.med.harvard.edu

(ASD) (*7*). Normal atrial partitioning requires sequential growth and resorption of a primitive septum (the septum primum) followed by the definitive, right-sided septum secundum (*8*). During embryogenesis, a hole is maintained between the atria, through which oxygenated blood is shunted so as to bypass the nonfunctional fetal lungs; this hole closes shortly after birth. The molecular signals that regulate cardiac septation are largely unknown, although recent genetic studies of a rare disorder, Holt-Oram syndrome (*9*), have shown that TBX5, a T-box transcription factor, plays a role. Conduction-system development occurs concurrently with cardiac septation (*8*), but the processes that specify organization of nodal structures or differentiation of specialized conduction cells are unknown. To investigate the molecular basis for these important cardiac morphogenetic events, we sought to identify the genetic defect that causes autosomal dominant ASD (secundum type) and atrioventricular conduction delays.

Four families, clinically followed by one of us, were known to have a high incidence of congenital heart disease. Clinical evaluations of surviving members (*10*) and pedigree analyses (Fig. 1A) demonstrated autosomal dominant transmission of this trait. Some 27 of 33 affected individuals had secundum ASDs (Fig. 2, A and B); all underwent surgical repair except for individual IV-4 (family MBF), whose defect spontaneously closed. Other structural heart malformations identified in affected individuals (Table 1) included ventricular septal defects, tetralogy of Fallot, subvalvular aortic stenosis, ventricular hypertrophy, pulmonary atresia, and redundant mitral valve leaflets with fenestrations.

Electrocardiograms demonstrated atrioventricular conduction delays in all individuals with congenital heart defects and in one individual with normal cardiac structures (*11*). Serial studies in some individuals indicated progressive conduction disease (Fig. 2C). Invasive electrophysiologic studies performed in individuals III-2, IV-4, and V-2 (family MBF) localized the prolonged conduction to the atrioventricular node (Fig. 2A); electrophysiologic properties of other conduction system components were normal. Pacemakers have been implanted in 14 affected individuals.

Cardiac deaths occurred in multiple affected individuals. Individuals IV-8, IV-10, and IV-12 (family MXP) died from complications of structural heart defects. In contrast, six asymptomatic individuals died suddenly (family MXP III-3; family MBT II-3, III-2; family MBX I-2, II-3, II-4). Each event occurred during adulthood, many years after surgical repair of an ASD. None had received a pacemaker.

Genome-wide linkage analyses (*12*) performed in family MXP demonstrated linkage to locus *D5S1456* [logarithm of the odds (LOD) score = 3.91, $\theta = 0$]. A common disease haplotype was identified in families MXP and MBF, suggesting that there was a founding mutation in a distant unknown ancestor of both kindreds. Analyses of flanking loci on chromosome 5q35 indicated that no recombination events had occurred in either families MBX or MBF at loci within 12 centimorgans of *D5S1456* or *D5S211* (*13*).

The gene encoding the homeobox transcription factor NKX2-5 (also called CSX) has been mapped to chromosome 5q35 (*14*) and to a yeast artificial chromosome containing *D5S211* (*15*). Given this protein's role in cardiac development in lower species (*3–5*), we hypothesized that mutations in *NKX2-5* might cause the congenital heart defects identified in the four study families. The genomic sequence of the human *NKX2-5* gene reported by other laboratories (*14, 16*) indicates that the gene consists of two exons and encodes a 324–amino acid protein (Fig. 3A). Using previously described primers (Fig. 3A) (*14*), we amplified and sequenced (*17*) both *NKX2-5* exons in DNA samples from two affected individuals in each study family.

Affected individuals in families MXP and MBF share a C→T transition at *NKX2-5* nucleotide 642, which is predicted to substitute a methionine codon (ATG) for the highly conserved threonine codon (ACG) at homeodomain position 41 (designated Thr178Met) (Fig. 3). Affected individuals in families MBT and MBX had sequence variants that encode truncated NKX2-5 proteins. A C→T transversion of nucleotide 618 (family MBT) is predicted to substitute a termination codon (TAG) for a glutamine (CAG) codon (designated Gln170ter), which

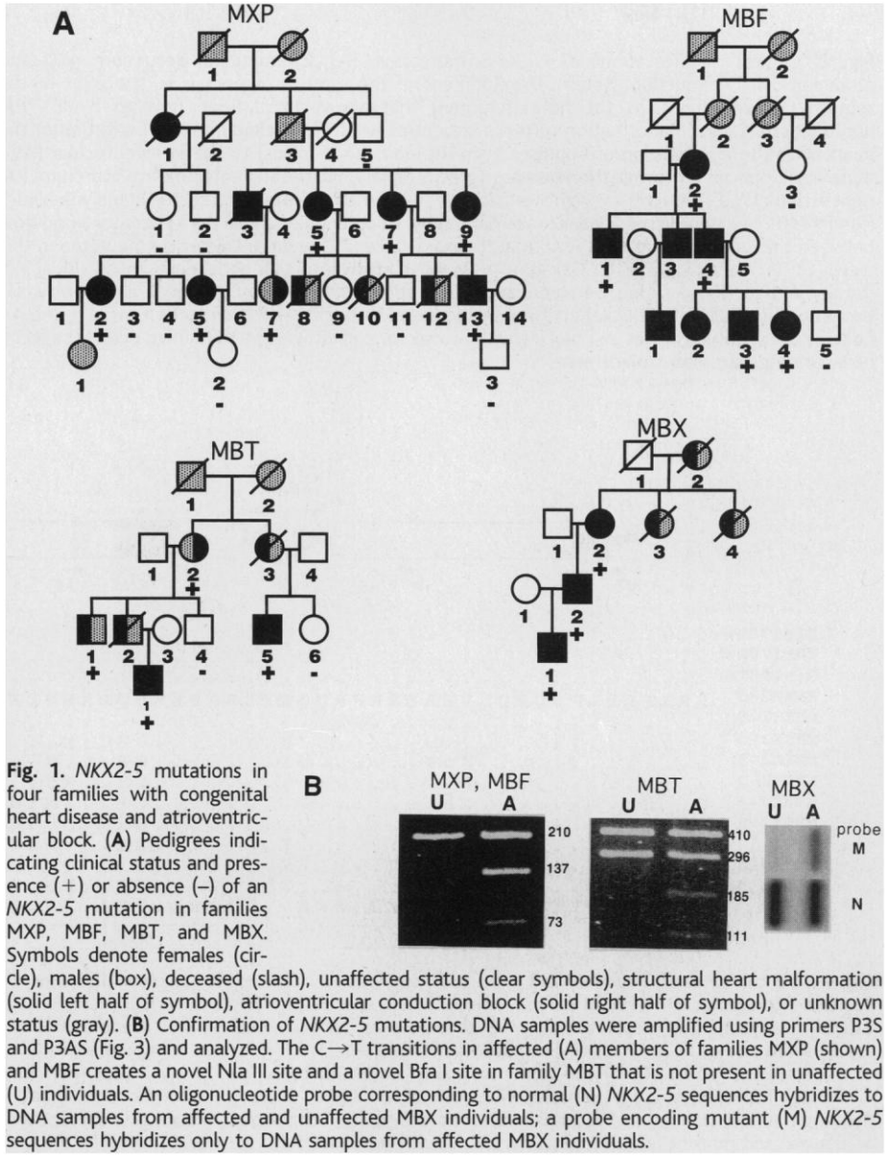

Fig. 1. *NKX2-5* mutations in four families with congenital heart disease and atrioventricular block. (**A**) Pedigrees indicating clinical status and presence (+) or absence (–) of an *NKX2-5* mutation in families MXP, MBF, MBT, and MBX. Symbols denote females (circle), males (box), deceased (slash), unaffected status (clear symbols), structural heart malformation (solid left half of symbol), atrioventricular conduction block (solid right half of symbol), or unknown status (gray). (**B**) Confirmation of *NKX2-5* mutations. DNA samples were amplified using primers P3S and P3AS (Fig. 3) and analyzed. The C→T transitions in affected (A) members of families MXP (shown) and MBF creates a novel Nla III site and a novel Bfa I site in family MBT that is not present in unaffected (U) individuals. An oligonucleotide probe corresponding to normal (N) *NKX2-5* sequences hybridizes to DNA samples from affected and unaffected MBX individuals; a probe encoding mutant (M) *NKX2-5* sequences hybridizes only to DNA samples from affected MBX individuals.

would stop translation prematurely at position 33 of the homeodomain. A C→T transversion at nucleotide 701 (designated Gln198ter; family MBX) is predicted to create a termination signal immediately COOH-terminal to the homeodomain.

Each sequence variant was independently confirmed by restriction enzyme digestion or oligonucleotide-specific hybridization (Fig. 1B). *NKX2-5* sequence abnormalities were present in DNA samples derived from all clinically affected but not unaffected members of study families (Fig. 1A) and were not present in more than 100 normal chromosomes from unrelated individuals (*13*). Linkage between the disease and each mutation was assessed in the study families, assuming an allele frequency of 0.01. Maximum LOD scores of 4.06 (family MXP), 1.23 (family MBF), 1.76 (family MBT), and 0.29 (family MBX) were achieved at $\theta = 0$.

The two mutations (Thr178Met and Gln170ter) within the DNA-binding homeodomain of NKX2-5 are likely to alter the affinity or sequence-specificity of target DNA binding, implying that NKX2-5 haploinsufficiency causes ASDs and atrioventricular node dysfunction. The Gln198ter mutation deletes COOH-terminal amino acids and is analogous in structure to a Nk2 box deletion construct (*18*) that increases transcription of reporter genes. Gln198ter may therefore function as an activating mutation that aberrantly augments transcription of downstream genes.

The viable cardiac malformations caused by human *NKX2-5* mutations (Table 1) are strikingly different from the early embryonic lethal defects observed in *Nkx2.5*-deficient mice (*5*) and the normal cardiac structures observed in heterozygote mutant mice. Although such differences may indicate distinct developmental pathways in mice versus humans, genetic redundancy, or unrecognized structural or electrophysiologic defects in heterozygous mice, these animal models may nonetheless reveal molecular signaling pathways that are relevant to human atrial septation. *Nkx2.5*-deficient mice fail to develop restricted, left-atrial expression of the basic helix-loop-helix factor, eHand (*19*). We speculate that induction of this left-right axial

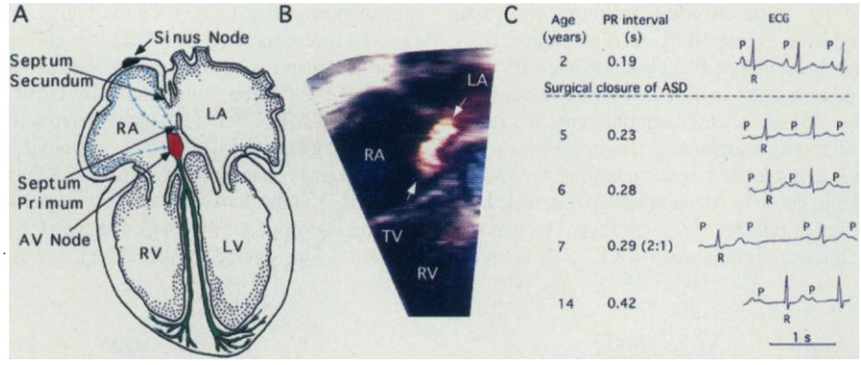

Fig. 2. Clinical manifestations of *NKX2-5* mutations. (**A**) Schematic of secundum ASD and atrioventricular conduction system. Development of the septum secundum to the right of the septum primum maintains the hole (foramen) that allows fetal blood flow to bypass the nonfunctional lungs. Malformation of these structures results in secundum ASD. Excitation of the heart occurs by propagation of impulses from the sinus node (black) to the atrioventricular (AV) node (red). Specialized conduction bundles (green) rapidly excite the ventricular myocardium. RA, right atrium; LA, left atrium; RV, right ventricle; LV, left ventricle. (**B**) ASD detected in individual III-5 (family MBT) by two-dimensional echocardiography. Doppler pulse signal (pink) detects blood flow between the left and right atria. A normal tricuspid valve (TV) and right ventricle are noted in this view. (**C**) Electrocardiograms (ECGs) show progressive atrioventricular nodal delay in individual V-4 (family MBF). The duration between atrial excitation (indicated by P wave) and ventricular excitation (indicated by R wave) abnormally increased through age 6. Conduction through the AV node at age 7 demonstrates 2:1 block (two P waves for each R wave) and marked delay at age 14, necessitating pacemaker placement.

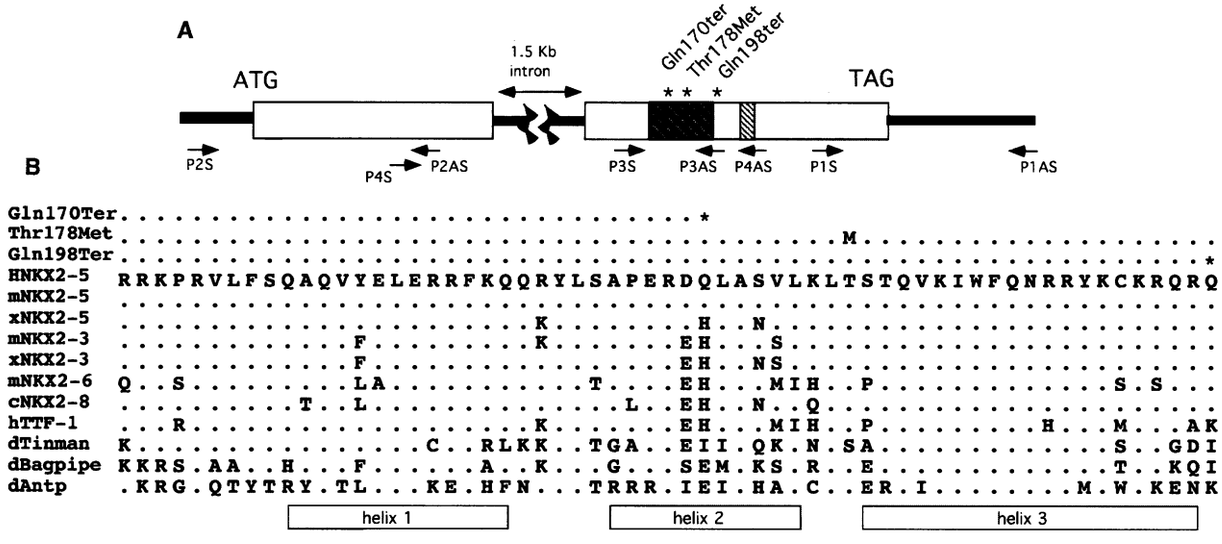

Fig. 3. Structure of the human *NKX2-5* gene, positions of mutations, and sequence comparison to related genes. (**A**) *NKX2-5* is encoded by two exons (open rectangles) separated by a 1.5-kb intron. Primer sequences are denoted and provided in (*14*). Mutations Gln170ter and Thr178Met alter sequences in helix 2 of the homeodomain (dark hatching). The Gln198ter mutation terminates translation just after helix 3, thereby deleting the COOH-terminal Nk domain (clear hatching). (**B**) Comparison of normal and mutant *NKX2-5* sequences (*21*) with homeodomain sequences in other *NK* gene family members and related genes: *thyroid nuclear factor-1* (TTF-1), *tinman*, *bagpipe*, and *antennapedia* (Antp) (*13, 16*). Gene names are prefixed with a species abbreviation in lower case: h, human; m, mouse; x, *Xenopus laevis*; c, chicken; and d, *Drosophila*. Dots denote identity; letters denote amino acid differences. Asterisks indicate termination signals. The Thr178Met defect alters a residue that is highly conserved in related genes. Three α helices within the homeodomain are indicated below the sequences.

system in humans by *NKX2-5* is important for specifying the precise location of atrial septum secundum development (to the right of the septum primum) (Fig. 2A) (*8*) and ultimately, appropriate atrial partitioning.

Elucidation of a critical role for Nkx2.5 in early cardiac specification and commitment in flies and mice (*2, 4*) may help to explain how *NKX2-5* mutations perturb human atrioventricular nodal function. In contrast to specialized fast-conducting fibers found in the ventricles, the atrioventricular node has few gap junctions and slowly propagates impulses (*20*). The electrophysiologic properties of the atrioventricular node are similar to those found in embryonic myocardium and may indicate that nodal cells are the vestigial remnants of primordial myocardial cells. We hypothesize that the cellular defects induced by *NKX2-5* mutations continue to be expressed in primitive atrioventricular nodal cells, but are masked in cells that have further evolved into the contractile myocardium or specialized conduction system.

The natural history of conduction-system disease in our study families delineates the importance of normal *NKX2-5* function during postnatal life. Progressive electrophysiologic abnormalities in individuals with normal heart structure or after spontaneous or surgical correction of ASDs (Table 1 and Fig. 2C) and a high incidence of sudden death in affected individuals without pacemakers indicate that normal amounts of NKX2-5 are required for physiologic atrioventricular node function throughout life. Characterization of the downstream targets of this transcription factor may explain why other myocardial cells are unaffected by *NKX2-5* defects and should further clarify the critical role of this gene in atrial and conduction tissue morphogenesis and maturation.

Table 1. Clinical features of affected individuals in families with congenital heart disease. Abbreviations: SVAS, subvalvular aortic stenosis; LVH, left ventricular hypertrophy; TOF, tetralogy of Fallot; PA, pulmonary atresia; VSD, ventricular septal defect; MVF, mitral valve fenestration; PM, pacemaker implanted; ⇓ 3 days, deceased age 3 days; ⇓ post-op, died post-operation; ⇓ HF, died of heart failure years after surgical correction of cardiac malformation; SD, sudden cardiac death; SC, spontaneous closure of ASD; AICD, automatic implanted cardiac defibrillator. + indicates presence of atrioventricular block; ? indicates that clinical data on atrioventricular block are not available.

Pedigree	ASD	Other structural defects	AV block	Comment
Family MXP				
II-1	+	–	+	PM
III-3	+	SVAS, LVH	+	SD
III-5	+	–	+	
III-7	+	–	+	PM
III-9	+	–	+	
IV-2	+	–	+	
IV-5	+	–	+	
IV-7	–	–	+	
IV-8	–	TOF, PA	?	⇓ 3 days
IV-10	+	VSD	?	⇓ post-op
IV-12	–	TOF	+	PM; ⇓ HF
IV-13	+	–	+	
V-1	–	VSD	?	
Family MBF				
III-2	+	–	+	PM
IV-1	+	–	+	PM
IV-3	+	–	+	
IV-4	+	–	+	PM, SC
V-1	+	–	+	PM
V-2	+	–	+	PM
V-3	+	–	+	PM
V-4	+	–	+	PM
Family MBT				
II-2	–	–	+	SD
II-3	+	–	?	
III-1	–	LVH	?	
III-2	+	–	?	SD
III-5	+	–	+	AICD
IV-7	+	–	+	
Family MBX				
I-2	+	–	?	SD
II-2	+	–	+	PM
II-3	+	LVH, MVF	?	SD
II-4	+	LVH	?	SD
III-2	+	–	+	PM
IV-1	+	–	+	PM

References and Notes

1. E. N. Olson and D. Srivastava, *Science* **272**, 671 (1996).
2. R. P. Harvey, *Dev. Biol.* **178**, 203 (1996).
3. M. C. Fishman and K. R. Chien, *Development* **124**, 2099 (1997).
4. R. Bodmer, *ibid.* **118**, 719 (1993).
5. I. Lyons *et al.*, *Genes Dev.* **9**, 1654 (1995).
6. I. Komuro and S. Izumo, *Proc. Natl. Acad. Sci. U.S.A.* **90**, 8145 (1993).
7. J. I. E. Hoffman, *Pediatr. Clin. North Am.* **37**, 25 (1990).
8. K. L. Moore and T. V. N. Persaud, *The Developing Human: Clinically Oriented Embryology* (Saunders, Philadelphia, 1998), pp. 349–404.
9. C. T. Basson *et al.*, *Nature Genet.* **15**, 30 (1997); Q. L. Li *et al.*, *ibid.*, p. 21.
10. W. E. Pease, A. Nordenberg, R. L. Ladda, *Circulation* **53**, 759 (1976); C. T. Basson *et al.*, *ibid.* **91**, 1326 (1995). Clinical evaluations and genetic studies were performed in accordance with human subject committee guidelines, without knowledge of genotype. Family members were studied by history, physical examination, 12-lead electrocardiogram, and two-dimensional transthoracic echocardiography with color flow Doppler interrogation in four standard and subcostal views.
11. Normal cardiac structures were confirmed by transthoracic and transesophageal echocardiographic examinations.
12. Linkage studies were performed using fluorescence-labeled polymorphic short tandem repeats (Weber set, version 8.0; Research Genetics), analyzed with an ABI 377 automated DNA sequencer. Alleles were assigned using Genescan version 2.0.2 software (ABI) and the Genotyper version 2.0 program. Two-point linkage analyses were calculated with the program MLINK version 5.1, assuming a disease penetrance of 0.95.
13. J.-J. Schott, C. E. Seidman, J. G. Seidman, unpublished data.
14. D. Turbay, S. B. Wechsler, K. M. Blanchard, S. Izumo, *Mol. Med.* **2**, 86 (1996).
15. M. Kostrzewa, D. L. Grady, R. K. Moyzis, L. Floter, U. Muller, *Hum. Genet.* **97**, 399 (1996).
16. I. Shiojima *et al.*, *Circ. Res.* **79**, 920 (1996).
17. Cycle sequencing reactions were performed in the presence of fluorescence-labeled dideoxynucleotides. Products were fractionated on an ABI 377 automated DNA sequencer, and analyzed using FACTURA (ABI) and SEQMAN (DNASTAR, Madison, WI) software.
18. C. Y. Chen and R. J. Schwartz, *J. Biol. Chem.* **270**, 15628 (1995).
19. C. Biben and R. P. Harvey, *Genes Dev.* **11**, 1357 (1997).
20. A. F. M. Moorman and W. H. Lamers, *Trends Cardiovasc. Med.* **4**, 257 (1994).
21. Single-letter abbreviations for the amino acid residues are as follows: A, Ala; C, Cys; D, Asp; E, Glu; F, Phe; G, Gly; H, His; I, Ile; K, Lys; L, Leu; M, Met; N, Asn; P, Pro; Q, Gln; R, Arg; S, Ser; T, Thr; V, Val; W, Trp; and Y, Tyr.

22. We thank B. McDonough and V. Friedenberg for help in patient studies and M. Miri and J. Soults for technical assistance. Supported by grants from the Fondation pour la Recherche Medicale (France), the Philippe Fondation (France), NIH, and the Howard Hughes Medical Institute.

6 April 1998; accepted 4 June 1998